Photoluminescence Properties of Novel Red-Emitting Mn^{2+}-Activated MZnOS (M = Ca, Ba) Phosphors

C. J. Duan, A. C. A. Delsing, and H. T. Hintzen*

Materials and Devices for Sustainable Energy Technologies, Department of Chemical Engineering and Chemistry, Eindhoven University of Technology, P.O. Box 513, 5600 MB Eindhoven, The Netherlands

Photoluminescence properties of novel red-emitting Mn^{2+}-activated MZnOS (M = Ca, Ba) phosphors were investigated. Mn^{2+}-activated MZnOS phosphors show a single symmetric narrow red emission band in the wavelength range of 550−700 nm due to the $^4T_1(^4G) \rightarrow {}^6A_1(^6S)$ transition of Mn^{2+}. Peak centers are at about 614 nm for M = Ca and 634 nm for M = Ba, regardless of the excitation wavelength and Mn^{2+} doping concentration. A comparison is made between the luminescence properties of Mn^{2+} in the Ca versus Ba compound. A similarity between them is that both Mn^{2+}-activated CaZnOS and BaZnOS can be efficiently excited under host lattice excitation in the wavelength range of 250−350 nm due to efficient energy transfer between the host lattice (MZnOS) and activator (Mn^{2+}). An unexpected difference is that Mn^{2+}-activated CaZnOS can also be efficiently excited under the excitation of Mn^{2+} itself (d−d transitions) in the wavelength range of 350−500 nm. This difference is ascribed to different crystal structures, different coordination environments, and point symmetries for Mn in these two compounds. The potential applications of these phosphors are pointed out. Among them, Mn^{2+}-activated CaZnOS shows great potential for application as an alternative red-emitting LED conversion phosphor due to its high absorption and strong excitation bands in the wavelength range of 350−500 nm.

1. Introduction

In recent years, great efforts have been made to investigate the luminescence properties of Mn^{2+}-activated Zn-based semiconductors. Among these ZnS,[1−6] ZnSe,[7] Zn_2SiO_4,[8−11] $ZnGa_2O_4$, [12,13]$ZnGa_2S_4$,[14,15] $SrZnO_2$,[16]Ba_2ZnS_3,[17−19] and BaZnOS [20]have been reported to be good host materials for Mn^{2+} luminescence. Structural investigations indicate that these host materials have some common characteristics. Their crystal structures all contain $[ZnX_4]$ (X = O, S, and Se) tetrahedrons. The transition metal activator (Mn^{2+}) can enter into the interior host lattice by replacing Zn^{2+} ion due to their similar ionic radii (The ionic radii of Mn^{2+} and Zn^{2+} are 0.80 and 0.74 Å, respectively.[21]) and charge. The wavelength position of the emission band of Mn^{2+} strongly depends on the host lattice because of the dependence on the crystal field. It can vary from green to deep red. Tetrahedrally coordinated Mn^{2+} (weak crystal-field) usually gives a green to yellow emission, whereas octohedrally coordinated Mn^{2+} (strong crystal-field) gives a red emission.[22] From the above-mentioned considerations, it can be anticipated that novel Zn-containing semiconductors with similar coordination environment of the $[ZnX_4]$ tetrahedron may be promising host materials for Mn^{2+}. The compound CaZnOS was first discovered by S. A. Petrova et.al. [23] in 2003 and subsequently its synthesis, structure, and electrical properties were investigated in detail by J. Clarke et al.[24] in 2007. The compound BaZnOS was first discovered by J. Clarke et al.[25] in 2006 and it has been very recently shown

* To whom correspondence should be addressed. Tel.: 31-40-2473113. Fax: 31-40-2445619. E-mail: h.t.hintzen@tue.nl.

(1) Bhargava, R. N.; Gallagher, D.; Hong, X.; Nurmikko, A. *Phys. Rev. Lett.* **1994**, *72*, 416.
(2) Tanaka, M. *J. Lumin.* **2002**, *100*, 163.
(3) Huang, J. M.; Yang, Y.; Xue, S. H.; Yang, B.; Liu, S. Y.; Shen, J. C. *Appl. Phys. Lett.* **1997**, *70*, 2335.
(4) Qi, L.; Lee, B. I.; Kim, J. M.; Jang, J. E.; Choe, J. Y. *J. Lumin.* **2003**, *104*, 261.
(5) Xu, S. J.; Chua, S. J.; Liu, B.; Gan, L. M.; Chew, C. H.; Xu, G. Q. *Appl. Phys. Lett.* **1998**, *73*, 478.
(6) Sun, L. D.; Liu, C. H.; Liao, C. S.; Yan, C. H. *Solid State Commun.* **1999**, *111*, 483.
(7) Suyver, J. F.; van der Beek, T.; Wuister, S. F.; Kelly, J. J.; Meijerink, A. *Appl. Phys. Lett.* **2001**, *79*, 4222.
(8) Bhatkar, V. B.; Omanwar, S. K.; Moharil, S. V. *Phys. Stat. Sol. (a)* **2002**, *191*, 272.
(9) Thiyagarajian, J.; Kottaisamy, M.; Ramachandra Rao, M. S. *J. Electrochem. Soc.* **2007**, *154*, H297.
(10) Xiong, L. M.; Shi, J. L.; Gu, J. L.; Li, L.; Huang, W. M.; Gao, J. H.; Ruan, M. L. *J. Phys. Chem. B* **2005**, *109*, 731.
(11) Sohn, K. S.; Cho, B.; Park, H. D. *J. Am. Ceram. Soc.* **1999**, *82* (10), 2779.
(12) Ohtake, T.; Sonoyama, N.; Sakata, T. *Electrochem. Commun.* **2005**, *7*, 1389.
(13) Tran, T. K.; Park, W.; Tomm, J. W.; Wagner, B. K.; Jacobsen, S. M.; Summers, C. J.; Yocom, P. N.; McClelland, S. K. *J. Appl. Phys.* **1995**, *78*, 5691.
(14) Yuta, M. M.; White, W. B. *J. Electrochem. Soc.* **1992**, *139*, 2347.
(15) Marsh, P. J.; Davies, D. A.; Silver, J.; Smith, D. W.; Withnall, R.; Vecht, A. *J. Electrochem. Soc.* **2001**, *148*, D89.
(16) Kubota, S.; Oyama, T.; Yamane, H.; Shimada, M. *Chem. Mater.* **2003**, *15*, 3403.
(17) Thiyagarajan, P.; Kottaisamy, M.; Ramachandra Rao, M. S. *J. Phys. D: Appl. Phys.* **2006**, *39*, 2701.
(18) Lin, Y. F.; Chang, Y. H.; Chang, Y. S.; Tsai, B. S.; Li, Y. C. *J. Alloys Compd.* **2006**, *421*, 268.
(19) Zhang, X. M.; Zeng, H. P.; Su, Q. *J. Alloys Compd.* **2007**, *441*, 259.
(20) Xia, Y. J.; Huang, F. Q.; Wang, W. D.; Wang, Y. M.; Yuan, K. D.; Liu, M. L.; Shi, J. L. *Opt. Mater.* **2008**, *31*, 311.
(21) Shannon, R. D. *Acta Crystallogr., Sect. A* **1976**, *32*, 751.
(22) Blasse, G.; Grabmaier, B. C. *Luminescent Materials*; Spring-Verlag: Berlin, 1994.
(23) Petrova, S. A.; Mar'evich, V. P.; Zakharov, R. G.; Selivanov, E. N.; Chumarev, V. M.; Udoeva, L. Yu. *Dokl. Chem.* **2003**, *393*, 255.
(24) Sambrook, T.; Smura, C. F.; Clarke, S. J.; Shi Halasyamani, P. *Inorg. Chem.* **2007**, *16*, 2571.
(25) Broadley, S.; Gál, Z. A.; Corá, F.; Smura, C. F.; Clarke, S. J. *Inorg. Chem.* **2005**, *44*, 9092.

10.1021/cm801990r CCC: $40.75
Published on Web 02/20/2009

Table 1. Comparison between the Crystal Structures of CaZnOS and BaZnOS

	CaZnOS	BaZnOS
space group	$P6_3mc$	$Cmcm$
host lattice band gap (eV)	3.71	3.9
volume per formula unit (Å^3)	69.69	77.89
number of Zn site	1	1
Zn coordination environment	ZnS_3O	ZnS_2O_2
average Zn−X (X = O, S) distance (Å)	2.254	2.157
Zn site point symmetry	C_{3V}	C_{2V}
ref	24	25

to be a good luminescent host lattice for doping with Mn^{2+} and Cu^+ ions.[20,26] However, no SrZnOS analogue has been reported yet. Both CaZnOS and BaZnOS have been shown to be a semiconductor with a band gap of about 3.71 and 3.9 eV, respectively. [24,25] The comparison between the crystal structures of CaZnOS and BaZnOS is given in Table 1. CaZnOS crystallizes in a hexagonal space group $P6_3mc$ with a = 3.75726 (3) Å, c = 11.4013 (1) Å, and Z = 2, whereas BaZnOS crystallizes in an orthorhombic space group $Cmcm$ with a = 3.9619 (2) Å, b = 12.8541 (7) Å, c = 6.1175 (4), and Z = 4.[24,25] Both crystal structures contain the above-mentioned [ZnX_4] tetrahedrons. In CaZnOS, each Zn is tetrahedally coordinated by three S atoms and an O atom (ZnS_3O) with C_{3v} point symmetry. The noncentrosymmetric structure of CaZnOS, which has only few analogues, is composed of isotypic puckered hexagonal ZnS and CaO layers arranged so that [ZnS_3O] tetrahedrons are all aligned parallel, resulting in a polar structure.[24] While in BaZnOS, each Zn is also tetrahedally coordinated by two S atoms and two O atoms (ZnS_2O_2) with C_{2V} point symmetry. The crystal structure of BaZnOS consists of vertex-linked [ZnO_2S_2] tetrahedral layers separated by Ba atoms.[25] All the structural characteristics suggest that MZnOS (M = Ca, Ba) may act as promising host lattices for Mn^{2+}. The good chemical and thermal stability of them are also very attractive. Therefore, it is worth to study the luminescence properties of Mn^{2+} in MZnOS (M = Ca, Ba) host lattices. As indicated above, each Zn atom is tetrahedrally coordinated in MZnOS (M = Ca, Ba) host lattices. Therefore, green-yellow emissions are expected for Mn^{2+} in these two host lattices. However, here we report unconventional luminescence properties for Mn^{2+} in MZnOS host lattices (i.e., red-emission combined with high UV-blue absorption, which are attractive properties for white LED applications) and discuss the relationship with structural characteristics.

2. Experimental Section

2.1. Synthesis of Undoped and Mn^{2+}-Doped MZnOS (M = Ca, Ba). Powder $MZn_{1-x}Mn_xOS$ ($0 \le x \le 0.2$) (M = Ca, Ba) samples were prepared by a solid-state reaction at high temperature. As for the preparation of Mn^{2+}-doped CaZnOS, $CaCO_3$, ZnS, and $MnCO_3$ were used as raw materials, whereas BaS, ZnO, and $MnCO_3$ were used as raw materials in the preparation of Mn^{2+}-doped BaZnOS. A large amount of secondary phases is formed by a solid-state reaction of $BaCO_3$, ZnS and $MnCO_3$ to prepare Mn^{2+}-doped BaZnOS samples, which is also true for the preparation of Mn^{2+}-doped CaZnOS samples by a reaction of CaS, ZnO and $MnCO_3$.

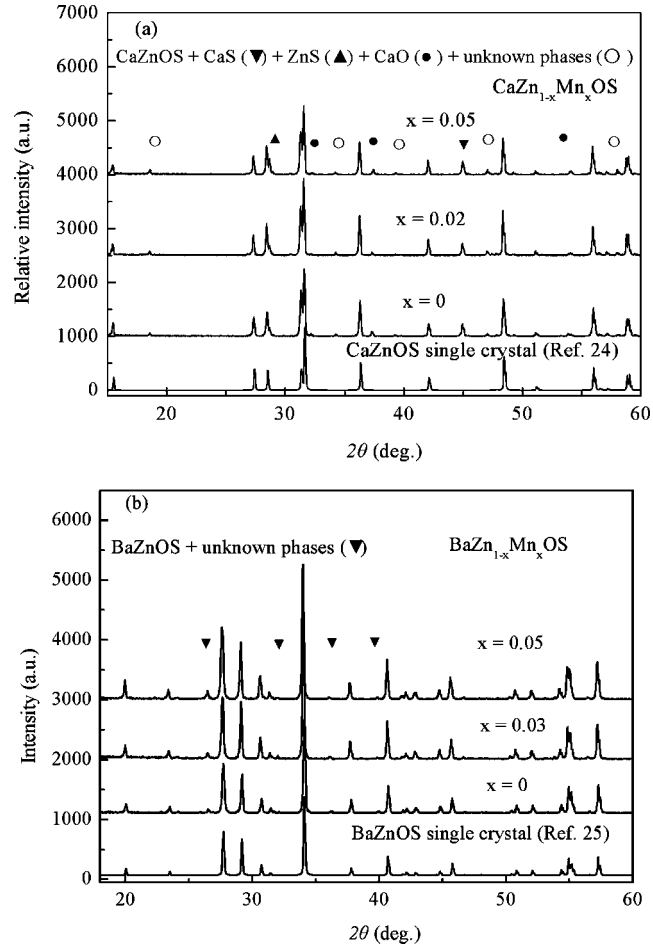

Figure 1. X-ray diffraction patterns of $MZn_{1-x}Mn_xOS$ powder samples: (a) M = Ca, (b) M = Ba.

The appropriate amounts of raw materials mentioned above were weighed out and subsequently mixed and ground together in an agate mortar. The powder mixtures were then transferred into molybdenum crucibles. All processes were carried out in a purified-nitrogen-filled glovebox. Subsequently, those powder mixtures were fired in a horizontal tube furnace at 920−1000 °C for 48 h under a flowing N_2 atmosphere. After firing, the samples were gradually cooled down to room temperature in the furnace. There was no apparent reaction of the prepared oxysulfide with the Mo crucibles.

2.2. X-ray Diffraction Data Collection. The XRD data for phase identification were collected at ambient temperature by X-ray powder diffractometer (Rigaku, D/MAX-B) with Cu Kα radiation operated at 40 kV and 30 mA with a scan speed of 0.6°/min in the 2θ range of 10−90°.

2.3. Optical Measurements. The diffuse reflectance, emission and excitation spectra of the samples were measured at room temperature in air by a Perkin-Elmer LS 50B spectrophotometer equipped with a Xe flash lamp. The reflection spectra were calibrated with the reflection of black felt (reflection 3%) and white barium sulfate ($BaSO_4$, reflection ~100%) in the wavelength region of 230−700 nm. The excitation and emission slits were set at 15 nm. The emission spectra were corrected by dividing the measured emission intensity by the ratio of the observed spectrum of a calibrated W lamp and its known spectrum from 300 to 900 nm. Excitation spectra were automatically corrected for the variation in the lamp intensity (and thus for the spectral dependence of the excitation energy) by a second photomultiplier and a beam splitter. All the luminescence spectra were measured with a scan speed of

(26) Xia, Y. J.; Huang, F. Q.; Wang, W. D.; Wang, A. B.; Shi, J. L. *Solid State Sci.* **2007**, *9*, 1074.

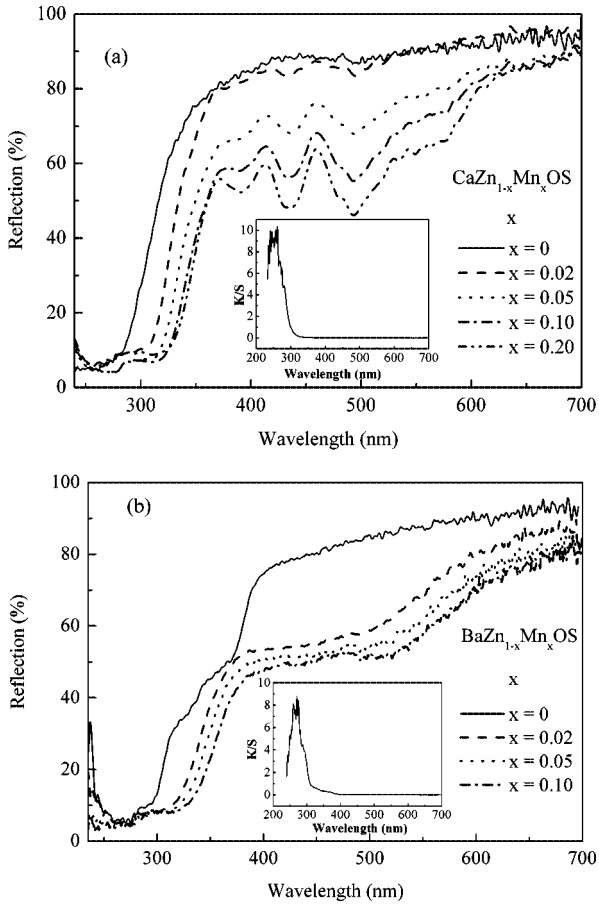

Figure 2. Diffuse reflection spectra of $MZn_{1-x}Mn_xOS$ powder samples: (a) M = Ca, (b) M = Ba.

400 nm/min. A commercial Zn_2SiO_4:Mn^{2+} (10%) sample (Philips) was included in the optical measurements for comparison.

3. Results and Discussion

3.1. Phase Formation. Panels a and b in Figure 1 show the powder XRD patterns of $CaZn_{1-x}Mn_xOS$ and $BaZn_{1-x}Mn_xOS$ ($0 \le x \le 0.05$) samples, respectively. By comparing these patterns with the calculated diffraction patterns obtained for the single crystals of CaZnOS and BaZnOS, respectively, $CaZn_{1-x}Mn_xOS$ phosphors are shown to be the main phase of the CaZnOS sample combined with a small amount of impurities, i.e. in particular CaS, plus ZnS, CaO, and some unknown phases. Compared to the reported preparation method using a sealed tube, relatively more impurities have been detected for our Mn^{2+}-doped CaZnOS samples,[23,24] while $BaZn_{1-x}Mn_xOS$ was formed as a nearly single phase material with only a trace of unknown secondary phases.

3.2. Diffuse Reflection Spectra of Undoped and Mn^{2+}-Doped MZnOS (M = Ca, Ba). Panels a and b in Figure 2 show the diffuse reflection spectra of undoped and Mn^{2+}-doped CaZnOS and BaZnOS samples, respectively. Both undoped and Mn^{2+}-doped MZnOS (M = Ca, Ba) samples show a strong drop in reflection in the UV range below 300 nm, corresponding to the valence-to-conduction band transitions of the MZnOS (M = Ca, Ba) host lattice. In order to better localize the threshold for host lattice absorption, the absorption spectra of CaZnOS and BaZnOS were obtained from the reflection spectra using the Kubelka−Munk function[27]

$$F(R) = (1 - R)^2 2/R = K/S \quad (1)$$

where R, K, and S are the reflection, the absorption coefficient and the scattering coefficient, respectively. The absorption spectrum (K/S) of MZnOS (M = Ca, Ba) derived with the Kubelka−Munk function is shown in the insets of Figure 2. The value of the optical band gap can be calculated by extrapolating the Kubelka−Munk function to $K/S = 0$. For undoped CaZnOS, there is only one absorption band with peak center at about 255 nm and its optical band gap is calculated to be about 4.0 eV (i.e., 310 nm), which is slightly larger than the previously reported value, i.e. 3.71 eV.[24] For undoped BaZnOS, two absorption bands can be observed. The main absorption band with peak center at about 270 nm is assigned to a direct band gap of 3.93 eV (i.e., 315 nm), which is in fair agreement with the value (3.93 eV)[25] from electronic structure calculations. The second one is the weak absorption at lower energy in the wavelength range of 320−400 nm, which is also observed for undoped and Cu^+-doped BaZnOS samples in the literatures,[25,26] and ascribed to impurity absorption because it is much more intense than absorption that would arise from indirect transitions. Additionally, the absorption edges of CaZnOS and BaZnOS show a minor red-shift with increasing Mn^{2+} concentration (Figure 2). A possible explanation can be ascribed to the increase of the lattice constants due to the incorporation of the larger Mn^{2+} into the MZnOS host lattice. An expanding host lattice will reduce the overlap between the oribitals of neighboring atoms. As a consequence, the splitting of the orbitals will decrease and so the distance between the valence and conduction bands. Because of its intense reflection in the visible spectral range, undoped CaZnOS shows a white daylight color, whereas undoped BaZnOS shows a light yellow color, which is related to the lower-energy absorption of impurities in the near visible spectral range. For Mn^{2+}-doped CaZnOS, obviously, several narrow strong absorption bands located at 396, 438, and 490 nm can be clearly seen from the reflection spectra of higher Mn^{2+} concentration samples. Due to the absence of them in undoped CaZnOS and the fact that the intensities increase for higher Mn^{2+} concentration, they obviously can be attributed to the absorption by Mn^{2+} ions. In contrast to the undoped sample, $CaZn_{1-x}Mn_xOS$ show white to pink color varying with the Mn^{2+} concentration. For Mn^{2+}-doped BaZnOS samples, they also show a strong absorption band in the wavelength range of 390−550 nm beside the main host lattice absorption band below 315 nm, which is in good agreement with pink color for Mn^{2+}-doped BaZnOS samples. However, as compared to Mn^{2+}-doped CaZnOS samples, the specific absorption bands of Mn^{2+} have not been observed at all in the visible range and no intensity dependence on the Mn^{2+} concentration is observed. Therefore, this absorption band probably is not related to the absorption by Mn^{2+} itself in the BaZnSO host lattice, in contrast to suggestions in the literature.[20] Figure 3 shows the comparison between the reflection spectrum of

(27) Yamashita, N. N. *J. Phys. Soc. Jpn.* **1973**, *35*, 1089.

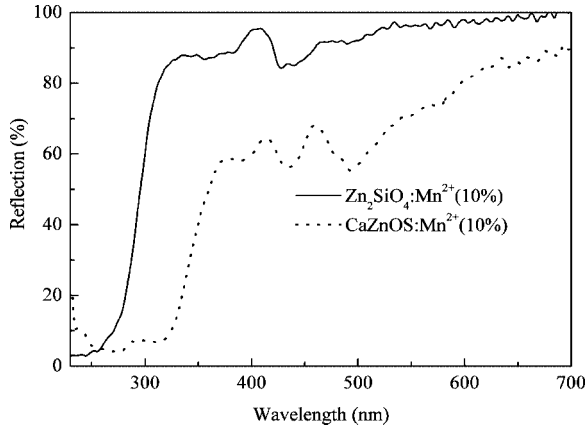

Figure 3. Comparison between the diffuse reflection spectrum of CaZnOS:Mn^{2+} (10 mol %) and that of commercial phosphor $Zn_2SiO_4:Mn^{2+}$ (10 mol %).

CaZnOS:Mn^{2+} (10%) and that of the commercial phosphor $Zn_2SiO_4:Mn^{2+}$ (10%). We can see that Mn^{2+} shows a relatively strong absorption in the wavelength range of 350−500 nm in CaZnOS as compared to the Zn_2SiO_4 host lattice. Because the d−d transitions of Mn^{2+} are spin and parity forbidden, the absorption bands of Mn^{2+} in CaZnOS are expected to be weak, as normally observed for Mn^{2+}, e.g., in Zn_2SiO_4 (Figure 3). On the contrary, the Mn^{2+} d−d transitions are rather intense in the CaZnOS host lattice. The unexpectedly strong absorption of Mn^{2+} in CaZnOS indicates that the spin and parity selection rules are shifted to a considerable extent. In the MZnOS:Mn^{2+} phosphor system, because the ionic size of M^{2+} (M = Ca, Ba) is much larger than that of Mn^{2+}, Mn^{2+} ions are expected to occupy the Zn^{2+} lattice sites (Mn_{Zn}) because of the similar ionic size (the ionic radii of Mn^{2+} and Zn^{2+} are 0.80 and 0.74 Å, respectively.[21]) and charge. As a consequence, Mn^{2+} is tetrahedrally coordinated with mixed O^{2-} and S^{2-} ions in MZnOS:Mn^{2+}. In the case of a significant degree of covalent bonding, the Mn^{2+} energy levels are no longer pure d states, but are mixed up with anion states with different parity. Mixing of states is easier for lower point symmetries, which is the case due to deviation from pure tetrahedral symmetry as a consequence of mixed $Mn(O,S)_4$ coordination in MZnOS:Mn^{2+}. In CaZnOS ($ZnOS_3$), the contribution of covalent bonding is higher than in BaZnOS (ZnO_2S_2), but for BaZnOS (point symmetry C_{2v}) the deviation from pure tetrahedral symmetry is higher than for CaZnOS (point symmetry C_{3v}). Because the absorption strength is particularly high for Mn^{2+}, the spin selection rule seems to be relaxed to some extent. This can be understood from the exchange interaction between the nearest neighbor Mn^{2+} ions, [28,29] which may also contribute to relaxing the parity selection rule.[30] This effect is expected to be more pronounced for CaZnOS as compared to BaZnOS because the volume per formula unit is significantly smaller for CaZnOS (69.69 $Å^3$) versus BaZnOS (77.89 $Å^3$),[24,25] inducing stronger interactions between the Mn^{2+} ions. As a consequence, Mn^{2+} itself shows a high absorption in the CaZnOS host lattice in the UV-blue range of the spectrum, which is important for use as a spectral conversion phosphor for white LED applications.

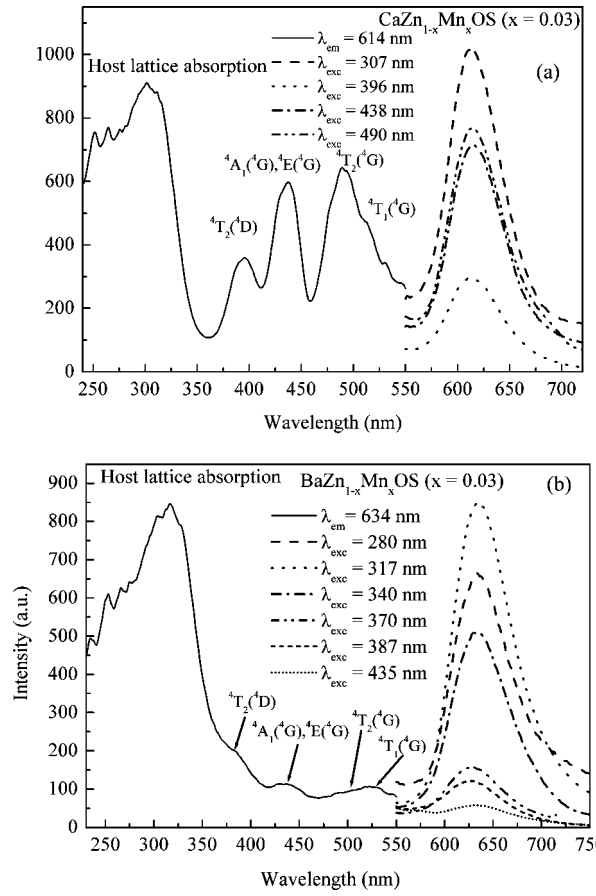

Figure 4. Typical excitation and emission spectra of $MZn_{1-x}Mn_xOS$ (x = 0.03) phosphors: (a) M = Ca, (b) M = Ba.

3.3. Photoluminescence Properties of Mn^{2+} in MZnOS (M = Ca, Ba). Panels a and b in Figure 4 show the excitation and emission spectra of $CaZn_{1-x}Mn_xOS$ and $BaZn_{1-x}Mn_xOS$ (x = 0.03) phosphors, respectively. Both of them show a narrow symmetric red emission band in the wavelength range of 550−700 nm with peak centers at about 614 and 634 nm for Mn^{2+}-doped CaZnOS and BaZnOS, respectively, regardless of the excitation wavelength. The observed band emission is ascribed to the $^4T_1(^4G) \rightarrow {}^6A_1(^6S)$ transition of Mn^{2+} incorporated in the MZnOS host lattice. In the crystal structure of MZnOS (M = Ca, Ba), there is only a single crystallographic site for Zn (Table 1), which is in good agreement with the observation of the single symmetric emission band of Mn^{2+} incorporated in the MZnOS host lattice. In addition, each Zn is tetrahedally coordinated. Normally green-yellow emission is observed for Mn^{2+} in a tetrahedral coordination environment, e.g., ZnS:Mn^{2+} (λ_{em} = 580 nm)[1] and $SrZnO_2:Mn^{2+}$ (λ_{em} = 575 nm).[16] As a consequence, green-yellow emissions are expected for Mn^{2+} in both CaZnOS and BaZnOS host lattices. However, unexpectedly, red emissions are observed for Mn^{2+} in both BaZnOS and CaZnOS host lattices. Normally, according to the Tanabe−Sugano diagram, a red Mn^{2+} emission is ascribed to the strong crystal field around the Mn^{2+} ion in the host lattice. A strong crystal field can be caused by: (1)

(28) Kolk, E.; van der; Dorenbos, P.; van Eijk, C. W. E.; Bechtel, H.; Jüstel, T.; Nikol, H.; Ronda, C. R.; Wiechert, D. U. *J. Lumin.* **2000**, *87−89*, 1246.
(29) Ronda, C. R.; Amrein, T. *J. Lumin.* **1996**, *69*, 245.
(30) Tanabe, Y.; Moriya, T.; Sugano, S. *Phy. Rev. Lett.* **1965**, *15*, 1023.

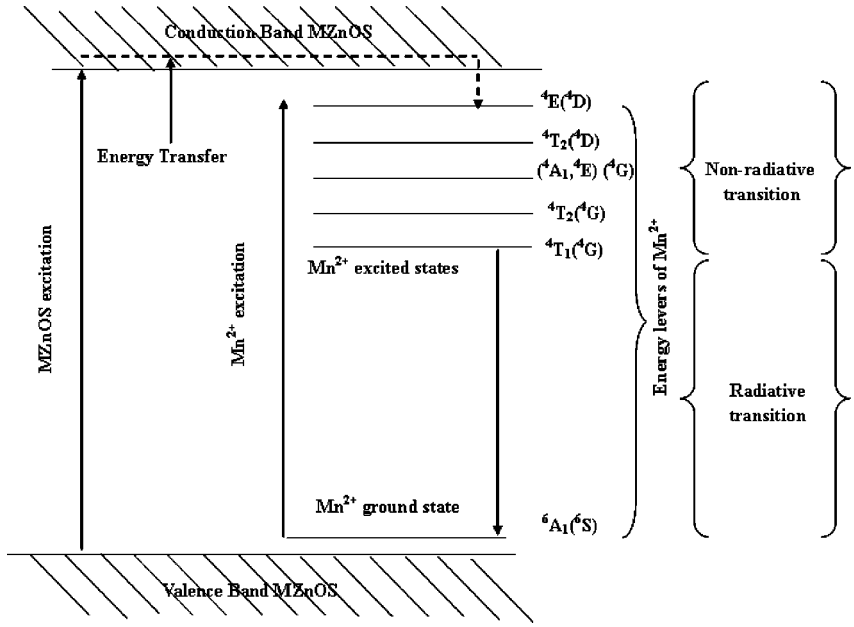

Figure 5. Idealized energy level scheme of MZnOS:Mn^{2+} phosphors (assuming pure tetrahedral point symmetry (T_d)).

higher charged coordinating ions (like for $MgSiN_2$:Mn^{2+} with N^{3-} ion); [31] (2) shorter Mn−X distances. The first possibility can be ruled out because Mn^{2+} is coordinated with O^{2-} and S^{2-} ions like in ZnS, Zn_2SiO_4, $SrZnO_2$, etc. In the crystal structure of CaZnOS, although the Zn−O distance (1.8996 Å)[24] is smaller than in ZnO (1.977 Å), [32] the Zn−S distance (2.3716 Å) is larger than in ZnS (∼2.34 Å),[33] resulting in the same average Zn-(O, S) distance (2.25 Å) as calculated from 3 × 2.34 Å (ZnS) and 1 × 1.977 Å (ZnO). In BaZnOS,[25] the Zn−S and Zn−O distances are equal to those in ZnS and ZnO, respectively, also resulting in the same average Zn−(O, S) distance. Therefore, the second possibility can also be ruled out. Because the crystal field effect can not explain the red emission observed for Mn^{2+} in MZnOS, it is ascribed to further splitting of the 2 level system of Mn^{2+} ion (*E* and *T* levels, valid for pure tetrahedral symmetry; point symmetry T_d) into more levels in a distorted tetrahedral coordination environment resulting in the first excited-state shifting to lower energy. For CaZnOS (Zn site point symmetry C_{3v}) splitting into 3 levels results: 2 E levels $\{[d_{(x^2-y^2)}, d_{xy}]$ and $(d_{xz}, d_{yz})\}$ and 1 A_1 level d_{z^2},[34] whereas for BaZnOS (Zn site point symmetry C_{2v}) a further splitting into five levels takes place: 2 A_1 levels $[d_{(x^2-y^2)}$ and $d_{z^2}]$, 1 A_2 level d_{xy}, 1 B_1 level d_{xz}, and 1 B_2 level d_{yz}.[34] As a consequence, the first excited-state of Mn^{2+} would be located at relatively lower energy in BaZnOS as compared to CaZnOS. Therefore, a longer-wavelength emission is observed for Mn^{2+} in BaZnOS (634 nm) than in CaZnOS (614 nm) host lattice.

The half-width for this single narrow emission band is about 50 nm for CaZnOS:Mn^{2+} and 60 nm for BaZnOS:Mn^{2+}, which resembles quite well with literature values for Mn^{2+}-doped phosphors, e.g., about 63 nm for ZnS:Mn^{2+} **1** and 60 nm for Ba_2ZnS_3:Mn^{2+} [17−19] The excitation spectra of both CaZnOS:Mn^{2+} and BaZnOS:Mn^{2+} (Figure 4) extend a broad range of wavelengths (230−550 nm) and are consistent with the diffuse reflectance spectra. Definitely, the short strong excitation bands below 350 nm originate from host lattice excitation as can be concluded from the corresponding drop in the reflection spectrum. The appearance of the strong host lattice excitation bands in the excitation spectrum of Mn^{2+} indicates that there exists efficient energy transfer from the MZnOS host lattice to Mn^{2+} ions. The remaining excitation bands in the wavelength range of 350−550 nm can be assigned to the transitions of Mn^{2+} from ground state $^6A_1(^6S)$ to the excited with term symbols given for ideal tetrahedral symmetry $^4T_2$ (^4D), [$^4A_1(^4G)$, $^4E(^4G)$], $^4T_2(^4G)$ and $^4T_1(^4G)$, respectively, as illustrated in Figure 4. Normally because d−d transitions of Mn^{2+} are spin and parity forbidden, the intensities of the excitation bands of Mn^{2+} itself are very weak as compared to those of the host lattice excitation bands. As a consequence, the emission intensities of such Mn^{2+}-doped phosphors are generally very weak for direct excitation of Mn^{2+} excitation levels. Such phenomenon has been observed in a lot of Mn^{2+}-doped phosphors, such as Zn_2SiO_4:Mn^{2+},[8−11] Ba_2ZnS_3:Mn^{2+},[17−19] $BaAl_{12}O_{19}$:Mn^{2+} [35] and $Zn_3(PO_4)_2$:Mn^{2+},[36] etc., and it is also true for Mn^{2+}-doped BaZnOS (Figure 4 b). However, for CaZnOS: Mn^{2+}, the intensities of the excitation bands of Mn^{2+} itself are rather strong (Figure 4 a) and the material can be efficiently excited in these Mn^{2+} bands, which can be ascribed to a high absorption and a high quantum efficiency of Mn^{2+} in the CaZnOS host lattice. The simplified energy level scheme and the main mechanisms involved in the generation of Mn^{2+} emission in MZnOS are shown in Figure 5. The typical band emission of Mn^{2+} in MZnOS host lattice can be realized in two different ways. The first way is to excite the Mn^{2+} ion directly in its own excitation levels. The electron from the ground-state of Mn^{2+} is excited into the higher energy levels of Mn^{2+}. Taking as a simplification pure tetrahedral point

(31) Duan, C. J.; Hintzen, H. T. To be published.
(32) Sawada, H.; Wang, R.; Sleight, A. W. *J. Solid State Chem.* **1996**, *122*, 148.
(33) Rabadanov, M.; Loshmanov, A. A.; Shaldin, Yu., V. *Kristallografiya* **1997**, *42*, 649.
(34) Atkins, P. W.; Child, M. S.; Philips, C. S. G. *Table for Group Theory*; University of Oxford: Oxford, U.K., 1970.
(35) Lee, D. Y.; Kang, Y. C.; Park, H. D.; Ryu, S. K. *J. Alloys Compd.* **2003**, *353*, 252.
(36) Wang, J.; Wang, S. B.; Su, Q. *J. Mater. Chem.* **2004**, *14*, 2569.

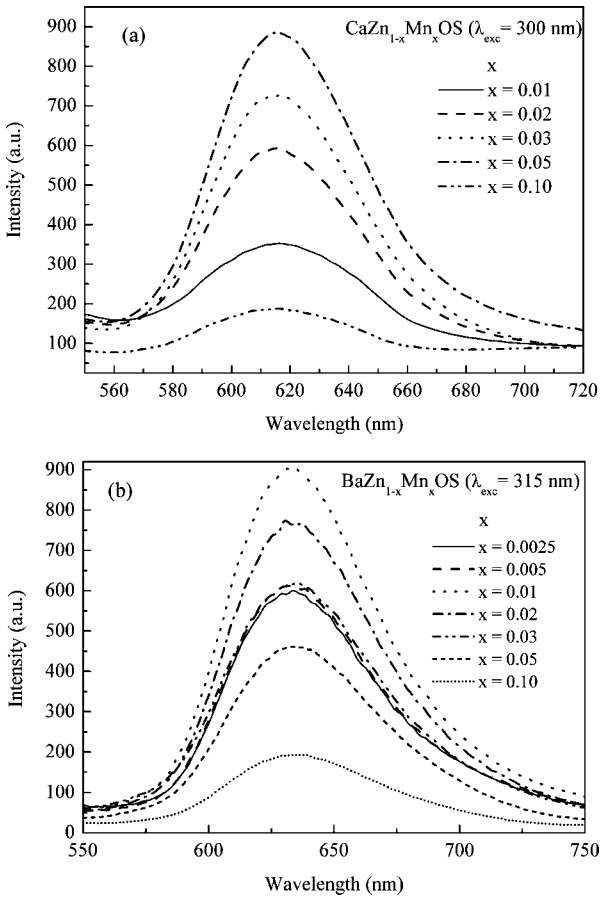

Figure 6. Emission spectra of $MZn_{1-x}Mn_xOS$ phosphors with different Mn^{2+} doping concentrations: (a) M = Ca, (b) M = Ba.

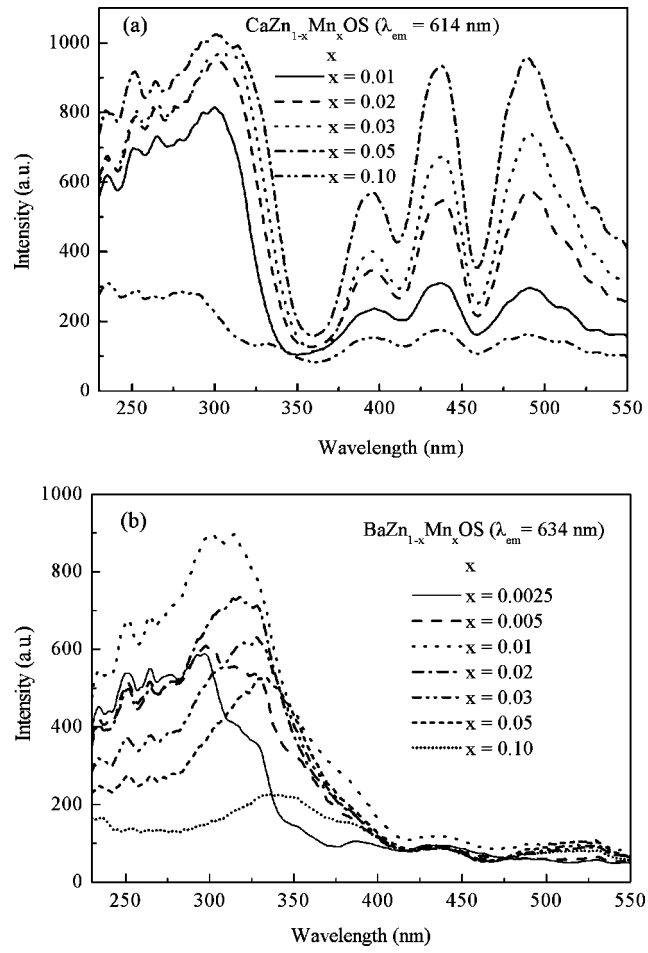

Figure 7. Excitation spectra of $MZn_{1-x}Mn_xOS$ phosphors with different Mn^{2+} doping concentrations: (a) M = Ca, (b) M = Ba.

symmetry, the excited free electron then relaxes to the $^4T_1(^4G)$ excited-state through $^4E(^4D)$, $^4T_2(^4D)$, $(^4A_1,^4E)(^4G)$, and $^4T_2(^4G)$ intermediate energy levels of Mn^{2+} by a nonradiative process, followed by a radiative transition from the $^4T_1(^4G)$ excited-state to the $^6A_1(^6S)$ ground-state giving rise the red emission of Mn^{2+} in the MZnOS host lattice. The second option is to excite first the host lattice, followed by efficient energy transfer from the host lattice to the Mn^{2+} ion, which also results in the typical emission of Mn^{2+}.

Panels a and b in Figure 6 show the emission spectra of $MZn_{1-x}Mn_xOS$ (M = Ba, Ca) phosphors as a function of the Mn^{2+} concentration. The position of the emission band of Mn^{2+} incorporated in the MZnOS host lattice is independent of the Mn^{2+} doping concentration. For Mn^{2+}-doped CaZnOS, the highest emission intensity is observed for the material doped with 5 mol % Mn^{2+} (i.e., $x = 0.05$) under excitation of host lattice. The emission intensity declines intensively as the concentration of Mn^{2+} exceeds 5 mol % because of concentration quenching. While the highest emission intensity is observed for the material doped with 1 mol % Mn^{2+} (i.e., $x = 0.01$) for Mn^{2+}-doped BaZnOS under excitation of host lattice. The above phenomenon is also true for the Mn^{2+}-doped MZnOS (M = Ca, Ba) for direct Mn^{2+} excitation.

Panels a and b in Figure 7 show the excitation spectra of CaZnOS:Mn^{2+} and BaZnOS:Mn^{2+} phosphors with different Mn^{2+} doping concentrations, respectively. The shape and position of the Mn^{2+} excitation bands are almost independent of the Mn^{2+} doping concentrations, whereas the Mn^{2+} doping concentration shows a great influence on the position of the host lattice excitation bands, especially for BaZnOS:Mn^{2+}. With increasing Mn^{2+} concentration, the peak centers of the host lattice excitation bands shifted to the longer-wavelength range, which is in good agreement with the diffuse reflection spectra of Mn^{2+}-doped MZnOS (M = Ca, Ba) (see Section 3.2), and ascribed to the increase of optical band gap with the incorporation of the larger Mn^{2+} into the MZnOS host lattice. Although the host excitation is independent of the luminescent center, the concentration of Mn^{2+} affects its excitation intensity intensely because this is also determined by energy transfer efficiency between the host lattice and Mn^{2+}. The maximum host lattice excitation intensity is obtained for the material doped with 5 mol % Mn^{2+} (i.e., $x = 0.05$) for M = Ca and 1 mol % Mn^{2+} (i.e., $x = 0.01$) for M = Ba. In addition, as expected, the ratio between the intensities of them (Mn^{2+} excitation bands/host lattice excitation bands) increases for increasing Mn^{2+} concentration, which can clearly seen from Figure 7a.

Table 2 summarizes the characteristics of MZnOS: Mn^{2+} (M = Ca, Ba) phosphors and compares them with some other typical Mn^{2+}-doped phosphors. From the comparison, we can see that Mn^{2+}-doped phosphors usually can only be efficiently excited for host lattice excitation instead direct excitation of the Mn^{2+} ion itself. The reason is that the Mn^{2+} excitation bands due to the d−d transitions of Mn^{2+} are spin-

Table 2. Characteristics of Mn^{2+}-Doped MZnOS (M = Ca, Ba) Phosphors As Compared to Those of Typical Mn^{2+}-Doped Phosphors at Room Temperature

phosphors	$Zn_2SiO_4:Mn^{2+}$	$Ba_2ZnS_3:Mn^{2+}$	$ZnS:Mn^{2+}$	$BaZn_{1-x}Mn_xOS$ ($0 \le x \le 0.2$)	$CaZn_{1-x}Mn_xOS$ ($0 \le x \le 0.2$)
cryst syst	*RH*	*Pnam*	$P6_3mc$	*Cmcm*	$P6_3mc$
body color	gray-white	gray-white	gray-white	light yellow to pink	white to pink
host lattice excitation bands (nm)	175, 250 (strong)	360 (strong)	332 (strong)	295−340 (strong)	290−310 (strong)
Mn^{2+} excitation bands (nm)	360, 380, 425, 440 (very weak)	410, 510 (very weak)	466, 498, 530 (very weak)	396, 438, 490 (very weak)	396, 438, 490 (strong)
emission peak center (nm)	520	625	585	634	614
full width at half-maximum broadband (nm)	40	60−70	63	60	50
ref	8	17−19	1, 2	20, this work	this work

and parity-forbidden, such as for $Zn_2SiO_4:Mn^{2+}$, $Ba_2ZnS_3:Mn^{2+}$, $ZnS:Mn^{2+}$, and $BaZnOS:Mn^{2+}$. However, $CaZnOS:Mn^{2+}$ can be efficiently excited not only under host lattice excitation but also for direct Mn^{2+} excitation, which can be ascribed to some lifting of the spin and parity prohibitions of Mn^{2+} d−d transitions in CaZnOS host lattice. So here, it is worth noting that $CaZnOS:Mn^{2+}$ has not only high absorption but also efficient excitation in the same spectrum range of 350−500 nm, matching with the radiative light from UV-blue LEDs. Thus, the luminescence properties of $CaZnOS:Mn^{2+}$ are favorable for white LED applications. As for the application for white LED, several kinds of Mn^{2+}-doped phosphors have already been reported, such as $Ba_2ZnS_3:Mn^{2+}$, [17−19] $LiZnPO_4:Mn^{2+}$,[37] and γ-$AlON:Mn^{2+}$,[38] etc. They show great potential for application as white LED conversion phosphors.

4. Conclusion

Novel red-emitting Mn^{2+}-activated MZnOS (M = Ca, Ba) phosphors have been prepared by a solid-state reaction method at high temperature and their photoluminescence properties were investigated. Mn^{2+}-activated MZnOS shows a single symmetric red emission band in the wavelength range of 550−700 nm with peak centers at about 614 nm for M = Ca and 634 nm for M = Ba, combined with half-widths of about 50 nm for M = Ca and 60 nm for M = Ba. The red emission observed for the tetrahedrally coordinated Mn^{2+} in MZnOS is ascribed to further splitting of the two-level system of Mn^{2+} ion into more levels in a distorted tetrahedral coordination environment resulting in the first excited-state shifting to lower energy. Due to the efficient energy transfer between host lattice and activator, both Mn^{2+}-activated CaZnOS and BaZnOS can be efficiently excited under host lattice excitation in the wavelength range of 230−350 nm. Moreover, Mn^{2+}-activated CaZnOS can also be efficiently excited by excitation of the Mn^{2+} ion itself in the wavelength range of 350−500 nm, which is uncommon for most Mn^{2+}-doped phosphors including Mn^{2+}-activated BaZnOS. This special behavior is ascribed to the lifting of the spin and parity prohibitions of Mn^{2+} d−d transitons in CaZnOS host lattice due to the derivation from pure tetrahedral symmetry as a consequence of mixed MnS_3O coordination with strong covalent bonding. The high absorption and strong excitation bands of $CaZn_{1-x}Mn_xOS$ in the wavelength range of 350−500 nm are very favorable properties for application as LED conversion phosphors. Generally speaking, this means that manipulating the coordination of the Mn^{2+} ion by taking mixed anions enlarge the opportunities for designing novel Mn^{2+}-doped phosphors with unconventional properties attractive for future white LED applications.

Acknowledgment. The authors thank M. M.R.M. Hendrix for his support with XRD measurements, H.A.M. van der Palen for maintenance of the furnaces, Dr. J. van Koesveld (Philips lighting) for providing the $Zn_2SiO_4:Mn^{2+}$ sample, and Leuchtstoffwerk Breitungen GmbH Company (Germany) for financial support.

CM801990R

(37) Chan, T. S.; Liu, R. S.; Baginskiy, I. *Chem. Mater.* **2008**, *20*, 1215.
(38) Xie, R. J.; Hirosaki, N.; Liu, X. J.; Takeda, T.; Li, H. L. *Appl. Phys. Lett.* **2008**, *92*, 201905.